

# Theoretical study of recoil-implanted N atoms in Mg-implanted GaN

Kai C. Herbert<sup>1</sup>, Kazuki Shibata<sup>1</sup>, Joel T. Asubar<sup>2</sup>, and Masaaki Kuzuhara<sup>1</sup>

<sup>1</sup>Kwansei Gakuin University, 2-1 Gakuen, Sanda, Hyogo 669-1337, Japan

<sup>2</sup>University of Fukui, 3-9-1 Bunkyo, Fukui, Fukui 910-8507, Japan

E-mail: [kcherbert@kwansei.ac.jp](mailto:kcherbert@kwansei.ac.jp), Phone: +81-80-4567-7963

**Keywords:** GaN, ion implantation, Magnesium (Mg), stoichiometry, Boltzmann transport equation

## Abstract

We calculated the depth distribution of implanted primary Mg ions and recoiled Ga and N atoms in a semiconductor by using a Boltzmann transport approach. It was found that the stoichiometric disturbance by Mg implantation was most significant for GaN, as compared to that for GaP, GaAs and GaSb. The peak density ratio (PDR), defined as the peak density of recoil-displaced group V atom with respect to that of group III atom, reached as high as 2.6 for GaN. Our calculation also proved that the PDR was rather insensitive to the changes in the implanted ion energy and the atom density in the target material. These results reveal that electrical activation of implanted Mg acceptors in GaN is more complicated and difficult than that in other semiconductors.

## INTRODUCTION

Ion implantation is recognized as a precise and high-yield doping technique. Thanks to its capability of selective-area doping, planar semiconductor structures can be prepared with well-defined lateral controllability for both p-type and n-type conductivities. In fact, it is widely used for the fabrication of various Si and SiC devices. Vertical GaN-based MOSFETs are attracting increased attention as low-loss and high-voltage power switching devices [1-3]. Magnesium (Mg) ion implantation into GaN is now extensively studied to make p-type channel layers as well as to achieve high-density p-type contact layers [4-10]. Optical characterization indicated formation of acceptor centers after thermal annealing of Mg-implanted GaN [4, 5]. However, except recent results using ultra-high-pressure annealing [6,7], only partial electrical activation has been reported on Mg-implanted GaN layers by using conventional activation annealing methods [8-10 oikawa2015, niwa2017, tanaka2019]. Contrary to the case for element semiconductors such as Si, it is predicted that ion implantation into GaN induces local stoichiometry imbalance in addition to generation of various point defects. Such additional difficulties might result in insufficient electrical activation of Mg acceptors implanted into GaN.

Christel and Gibbons proposed an efficient algorithm to calculate the momentum distributions of moving atoms in the material by using Boltzmann transport equation [11,12]. In this method, distribution functions of moving atoms,

including both primary and recoil-implanted atoms, are numerically solved with respect to the depth from the semiconductor surface, thus enabling the calculation of redistributed atoms in the target material. In this way, one can calculate in-depth local imbalance of stoichiometry after ion implantation.

In this work, we have applied this approach to Mg-implanted GaN and calculated the momentum distributions of recoil-implanted Ga and N atoms. As a result, it was found that the implantation-induced stoichiometry disturbance became most significant in GaN, as compared to that induced in other III-V compound semiconductors. Possible mechanisms for the stoichiometry imbalance are discussed.

## CALCULATION PROCEDURE

Following the approach proposed by Christel and Gibbons [11,12], momentum distributions of moving atoms, including primary and recoil-implanted atoms were calculated stepwise as a function of the depth  $z$  based on the Boltzmann transport equation:

$$\frac{\partial F(\mathbf{p})}{\partial z} = N \int \left( \frac{F(\mathbf{p}') d\sigma(\mathbf{p}' \rightarrow \mathbf{p})}{\cos\theta_{p'}} - \frac{F(\mathbf{p}) d\sigma(\mathbf{p} \rightarrow \mathbf{p}')}{\cos\theta_p} \right) + Q(\mathbf{p})$$

Here,  $F(\mathbf{p})$  denotes the momentum distribution function of atoms with momentum  $\mathbf{p}$ , and  $d\sigma$  is the scattering cross section. In our calculation, momentum  $\mathbf{p}$  was represented by the kinetic energy  $E$  of the atom and the angle  $\theta$  of its moving direction with respect to the target surface normal direction.  $Q(\mathbf{p})$  is the generation term, corresponding to the distribution of recoil atoms created from rest. The target material was assumed amorphous. The depth dependent distribution function of each atom is schematically illustrated in Fig. 1.

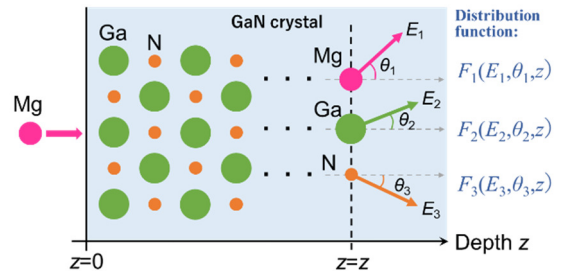


Fig. 1 Illustration of distribution functions of atoms.

Nuclear collisions (elastic) and electronic stopping process (inelastic) were considered as two independent scattering mechanisms. The elastic nuclear event was assumed as classical two-body mechanics, in which angular deflections of both incident and recoil atoms occurred with energy transfer between those atoms. Thus, only nuclear events generated recoil atoms. For the elastic nuclear cross section, we adopted the hybrid formula proposed by Christel and Gibbons [11,12].

Each atom was assumed stopped when its kinetic energy was reduced to nearly zero ( $E < E_s$ ) or when it was directed toward the semiconductor surface. The range distributions of both primary and recoil particles were thus determined at each depth.

### RESULTS

Figure 2 shows the concentrations of vacancies and displaced atoms of Ga and N as a function of the depth, together with the implanted Mg atom profile (220 keV,  $10^{15} \text{ cm}^{-2}$ ). Open squares and triangles indicate a net vacancy concentration, while closed squares and triangles indicate a net displaced atom concentration. Note that a high density of vacancies (Ga and N) is introduced in the shallow region, while recoil atoms are accumulated in the deeper region. The projected range was defined as the depth of the peak concentration for the implanted Mg. This projected range is  $0.21 \mu\text{m}$  by our calculations, although SRIM software calculations suggest a slightly larger range of  $0.26 \mu\text{m}$ . By comparing the effect of recoil implantation for Ga and N atoms, the N atoms have a much larger concentration in both profiles of vacancy and displaced atoms. When the peak density ratio (PDR) is defined as the peak density of displaced N divided by that of displaced Ga, it reaches as high as 2.6. Considering that implanted Mg should occupy Ga sites as

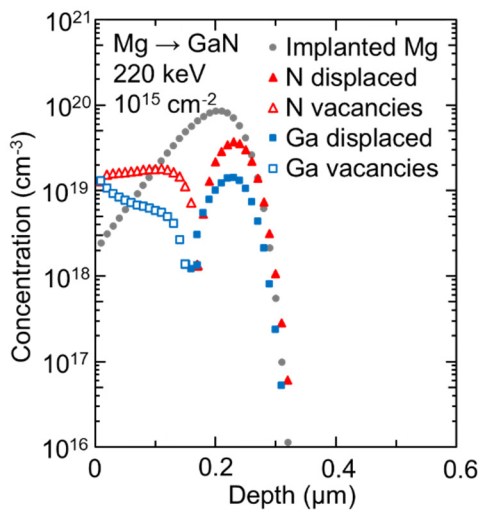


Fig. 2. Stoichiometric distribution in GaN implanted with 220 keV Mg.

acceptors, the formation of much higher density of N vacancies in the shallow region (less than  $0.15 \mu\text{m}$ ) is not beneficial for achieving increased electrical activation by Mg implantation into GaN.

Figures 3 and 4 show the concentrations of vacancies and displaced atoms as a function of the depth, together with the implanted Mg atom profile (220 keV,  $10^{15} \text{ cm}^{-2}$ ) in GaAs and GaSb. For GaAs, there is not a large concentration difference between Ga and As atoms. For GaSb, the concentration of Sb appears to be lower than the profile of Ga. When the PDR is similarly calculated as the peak density of displaced group V atoms (As and Sb) divided by that of displaced Ga, it reaches 1.0 and 0.7.

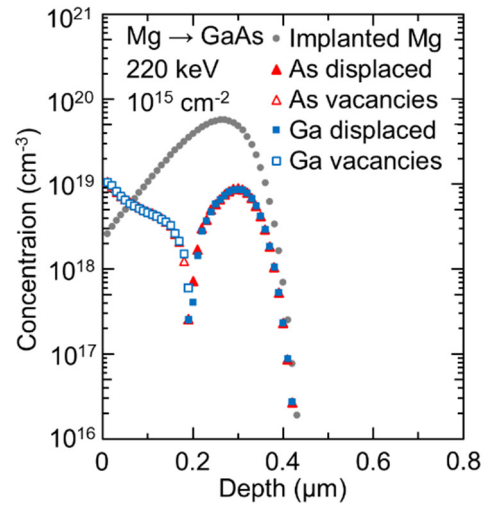


Fig. 3. Stoichiometric distribution in GaAs implanted with 220 keV Mg.

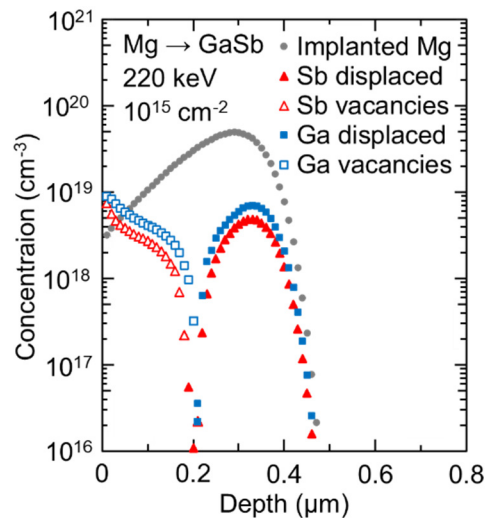


Fig. 4. Stoichiometric distribution in GaSb implanted with 220 keV Mg.

Figure 5 shows the calculated PDR as a function of the atom number of group V atoms in III-V semiconductors. The results show that PDR decreases with the increase in the group V atom number, indicating the PDR is the highest in GaN as compared to that in other III-V materials, such as GaP, GaAs and GaSb. In other words, the induced stoichiometric disturbance (N-rich) becomes most significant in GaN. We have also performed similar calculations by changing the primary Mg ion energy from 100 to 330 keV. However, it was found that the trend of PRD was calculated to be essentially the same as that in Fig.5 with only a small deviation of 3 %.

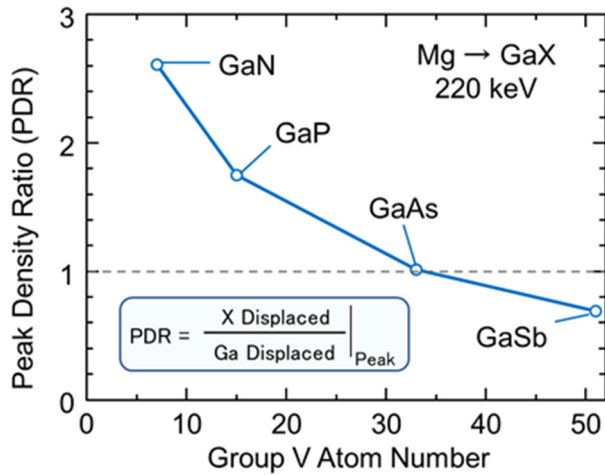


Fig. 5. Peak density ratio of displaced group III and V atoms as a function of group V atom number for GaN, GaP, GaAs, and GaSb.

#### DISCUSSION

For PDR calculation, each atom density was precisely chosen for GaN, GaP, GaAs and GaSb as  $8.8 \times 10^{22}$ ,  $4.9 \times 10^{22}$ ,  $4.6 \times 10^{22}$ ,  $3.5 \times 10^{22}$   $\text{cm}^{-3}$ , respectively. From Fig.5, we see that the atom density gradually decreases with increasing the atom number. To see if the decrease in PDR is attributed to the atom density, the atom density was fixed at  $8.8 \times 10^{22}$   $\text{cm}^{-3}$  (corresponding to the atom density of GaN) and the PDR was again calculated. Nevertheless, the PDR results were almost unchanged with only a slight deviation of 4%. In other words, the effect of the target material atom density on PDR is almost negligible.

To see how group V atoms affect the formation of PDR, similar calculation was performed while artificially varying the group V atom number (or atom weight). Figure 6 shows the calculated PDR as a function of the atom number of group V atom. In this calculation, the atom density was fixed at  $8.8 \times 10^{22}$   $\text{cm}^{-3}$ . Contrary to the initial expectation, PRD was found to saturate and decrease when the group V atom number was virtually reduced to less than 7, which corresponds to the atom number of N atom.

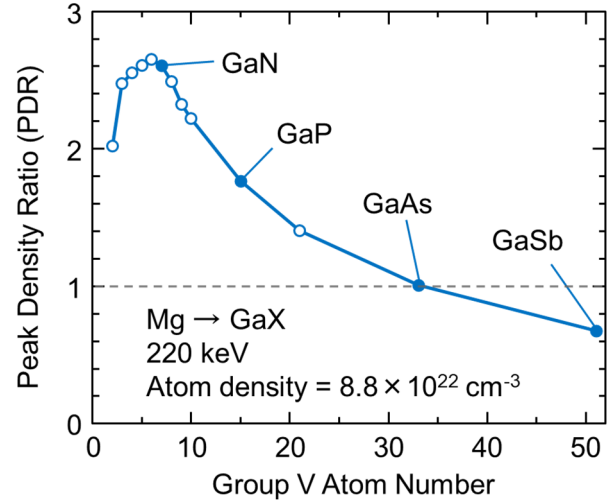


Fig. 6. Peak density ratio of displaced group III and V atoms as a function of group V atom number for GaX.

Figure 7 shows the calculated concentrations of recoil-displaced atoms as a function of the depth, together with the implanted Mg atom profile in GaX. Here, GaX is an artificial semiconductor material composed of Ga as a group III atom and X as a group V atom. When the atom number of X is 4 ( $Z_X=4$ ), the displaced X atom profile shifts to a deeper range, as compared to the implanted Mg. On the other hand, when the atom number X is 10 ( $Z_X=10$ ), the displaced X atoms are within the Mg profile. With a lighter atom number of X, the displaced X atoms become easier to move into a deeper region. This may presumably be the reason why PDR presented a saturated trend around an atom number of 7 and then started to decrease again when the atom number of X was further decreased to less than 7.

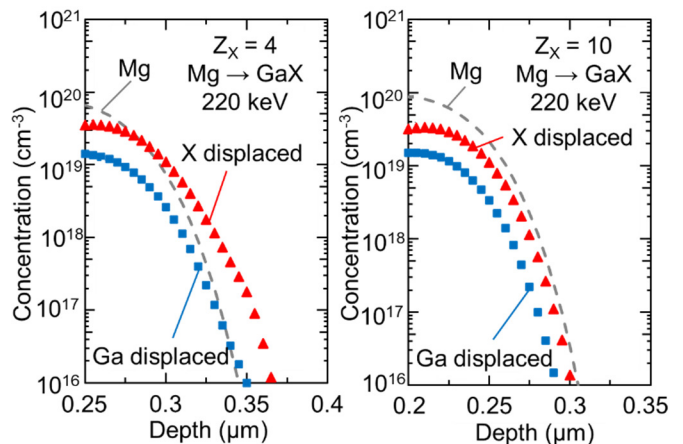


Fig. 7. Recoil-displaced atom distribution in GaX for  $Z_X=4$  and  $Z_X=10$ .

## CONCLUSIONS

We used a Boltzmann transport approach to calculate the depth distribution of implanted primary Mg ions and the recoiled Ga and N atoms. As a result, we found that the stoichiometric disturbance is significant for Mg implanted GaN, comparing it with GaP, GaAs and GaSb. The peak density ratio of the displaced Ga and N reached 2.6. Also, we found that the stoichiometric disturbance is insensitive to the change in the implanted ion energy and the target material atom density. Among various III-V materials investigated, Mg implantation into GaN revealed the largest stoichiometric disturbance, making the formation of p-type GaN by Mg implantation more complicated and difficult than other semiconductors.

## REFERENCES

- [1] I. C. Kizilyalli, A. P. Edwards, O. Aktas, T. Prunty, and D. Bour, *IEEE Trans. Electron Devices* 62, 414 (2015).
- [2] M. Kodama, M. Sugimoto, E. Hayashi, N. Soejima, O. Ishiguro, M. Kanechika, K. Itoh, H. Ueda, T. Uesugi, and T. Kachi, *Appl. Phys. Express* 1, 021104 (2008).
- [3] T. Oka, Y. Ueno, T. Ina, and K. Hasegawa, *Appl. Phys. Express* 7, 021002 (2014).
- [4] B. N. Feigelson, T. J. Anderson, M. Abraham, J. A. Freitas, J. K. Hite, C. R. Eddy, and F. J. Kub, *J. Cryst. Growth* 350, 21 (2012).
- [5] T. Narita, T. Kachi, K. Kataoka, and T. Uesugi, *Appl. Phys. Express* 10, 016501 (2017).
- [6] H. Sakurai, M. Omori, S. Yamada, Y. Furukawa, H. Suzuki, T. Narita, K. Kataoka, M. Horita, M. Bockowski, J. Suda, and T. Kachi, *Appl. Phys. Lett.* 115, 142104 (2019).
- [7] H. Sakurai, T. Narita, M. Omori, S. Yamada, A. Koura, M. Iwinska, K. Kataoka, M. Horita, N. Ikarashi, M. Bockowski, J. Suda, and T. Kachi, *Appl. Phys. Express* 13, 086501 (2020).
- [8] T. Oikawa, Y. Saijo, S. Kato, T. Mishima, and T. Nakamura, *Nucl. Instrum. Methods Phys. Res. Sect. B* 365, 168 (2015).
- [9] T. Niwa, T. Fujii, and T. Oka, *Appl. Phys. Express* 10, 091002 (2017).
- [10] R. Tanaka, S. Takashima, K. Ueno, H. Matsuyama, M. Edo, and K. Nakagawa, *Appl. Phys. Express* 12, 054001 (2019).
- [11] L. A. Christel, J. F. Gibbons, and S. Mylroie, *J. Appl. Phys.* 51, 6176 (1980).
- [12] L. A. Christel and J. F. Gibbons, *J. Appl. Phys.* 52, 5050 (1981).

## ACRONYMS

MOSFET: Metal-Oxide-Semiconductor Field-Effect Transistor

GaN: Gallium Nitride

GaP: Gallium Phosphide

GaAs: Gallium Arsenide

GaSb: Gallium Antimonide

PDR: Peak Density Ratio